Multi-Step Sensor Management for Localizing Movable Sources of Spatially Distributed Phenomena

Achim Kuwertz[1,2], **Marco F. Huber**[1,2]
[1] Institute for Anthropomatics
Karlsruhe Institute of Technology (KIT)
Karlsruhe, Germany
achim.kuwertz@kit.edu, marco.huber@ieee.org

Felix Sawo[2]
[2] Fraunhofer Institute of Optronics, System Technologies and Image Exploitation IOSB
Karlsruhe, Germany
felix.sawo@iosb.fraunhofer.de

Abstract – *Localizing sources of physical quantities is often only possible in an indirect manner by observing the induced continuous phenomena, such as pollution loads of air or water. By employing model-based reconstruction methods, the task of localizing movable sources by distributed sensor measurements can be formulated as a non-linear stochastic parameter estimation problem. A computationally efficient state estimator is applied to this estimation problem for enabling real-time source localization. Furthermore, this paper proposes a novel approach to multi-step sensor management for utilizing future sensors measurements in a most informative way. Here, predictive statistical linearization is employed for converting the given non-linear non-Gaussian sensor management problem into a linear Gaussian one, which can be solved efficiently. By controlling a mobile sensor, it is demonstrated that the proposed method yields accurate source localization results.*

Keywords: Source localization, target tracking, non-linear state estimation, sensor scheduling, mobile sensor control.

1 Introduction

Spatially distributed phenomena can be encountered on numerous occasions in man-made or natural surroundings. Examples of such phenomena are given by contaminations of air and water, e.g., leaking gases or marine oil spills, as well as temperature distributions over vast areas or in confined spaces. Including spatial distributions of harmful physical quantities, these phenomena can negatively impact both man and nature. Monitoring spatially distributed phenomena by automated sensor systems is thus a beneficial task. For example, the hazardous impact of pollution loads can be significantly reduced if they are detected early.

Spatially *distributed sensing systems* are well suited for the observation of distributed phenomena due to the continuous nature and spatial extensions of these phenomena. Recent developments in wireless communication and sensor technologies facilitate the usage of sensor systems like *sensor networks* [1] or *teams of mobile sensing robots*. Distributed sensors perform measurements at different spatial locations and distinct points of time, leading to isolated measurement values at discrete points in space and time.

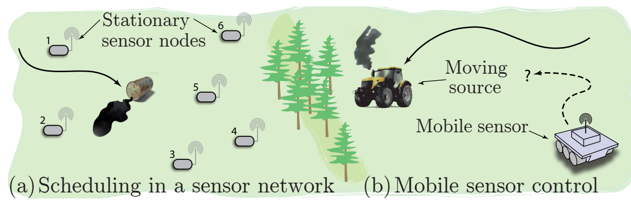

Figure 1: Localization of a movable source by (a) a network of stationary sensor nodes or (b) mobile sensing robots.

Distributed phenomena, however, are characterized by a *continuous variation* in time and space, meaning, for example, a continuous change with elapsing time. In order to accurately acquire and represent spatially distributed phenomena, it is therefore necessary to reconstruct a continuous distribution based on the acquired discrete phenomenon values. For this purpose, a *model-based reconstruction* approach as illustrated in Section 2 is employed in this paper.

Movable Source Localization and Tracking Within the area of monitoring spatially distributed phenomena, source localization [2, 3, 4] has been subject of ongoing research. In source localization, the location of a phenomenon source is estimated by measuring the distribution of the emitted physical quantities. In contrast to *direct* measurement methods for localization like distance or angular measurements, information about the location of a source can only be gathered *indirectly* by observing the induced distributed phenomenon. This in particular makes source localization a complex and challenging problem.

As an extension to this problem, *localization and tracking of movable sources* is considered in this paper. This extension specifically copes with the problem of how to efficiently locate and track non-stationary sources of continuously distributed phenomena by selective space-time measurements, as depicted in Figure 1. In Section 3 of this paper, a model-based approach for localizing movable sources by means of stochastic estimation methods is introduced.

Sensor Management Another extension to the source localization and tracking problem is given by the task of *controlling* the employed sensor system by means of *sensor management*. Sensor management thereby allows for maximizing the information gain of performed measurements. Hence, the number of measurements required to locate and track a phenomenon source is decreased. In a stationary sensor network, e.g., sensor scheduling (see Fig. 3(a)) allows for reducing the number of simultaneously active nodes and thus, saves energy resources. For mobile sensors, localization performance can be enhanced by employing mobile sensor control (see Fig. 3(b)) for path planning [5, 6].

In this paper, the following *scenario* for an exemplary source localization is considered: in a confined area, for example a storage facility for chemicals, the release of an airborne contaminant has been detected. In order to avoid threats to human lives, mobile sensing robots are used, each equipped with sensors for measuring the contaminant concentration at its current location. The task of these robots is hence to identify, to locate and to track the contamination source by moving and measuring within the given area. In Section 4, a *sensor management approach* is presented, suitable of supporting sensor scheduling and mobile sensor control for source localization.

2 Model-Based Reconstruction

A spatially distributed phenomenon describes a continuous distribution of physical quantities in space, which continuously vary over time. In an exact mathematical formulation, these phenomena are represented as a continuous function $p(\underline{z}, t)$ of space and time, with $\underline{z} \in \mathbb{R}^2$ or $\underline{z} \in \mathbb{R}^3$ being a spatial location and $t \in \mathbb{R}^+$ denoting a point in time.

As a prerequisite for successfully locating a phenomenon source, an adequate acquisition of information about the induced phenomenon is necessary. By utilizing a distributed sensor system for information acquisition, selective measurements such as concentration values can be gathered. These sensor systems are therefore only able to *discretely sample* a continuous phenomenon at isolated locations and at single points of time. For phenomenon values at points in space and time that do not correspond to measurement points, no direct information is available.

For avoiding high sampling rates in the spatial and temporal domain, phenomenon values at non-measurement points can be gained by the utilization of interpolation techniques. In this paper, a *model-based reconstruction* [7, 8] approach is employed for this purpose. This enables not only a spatial interpolation but also allows for a temporal synchronization of measurement values. At the heart of this approach, a mathematical model of the considered continuous phenomenon serves as a basis for all calculations.

A large number of spatially distributed phenomena can be described by means of a system of partial differential equations *(PDE)*. This paper focuses on the subset of two-dimensional linear phenomena, which for example includes *advection-diffusion reactions* and *heat conduction processes*. A general mathematical model of such phenomena is given by a linear partial differential equation without cross-derivatives. Using the linear operator $\mathbb{L}(\,\cdot\,)$, this linear PDE can be stated as

$$\mathbb{L}\bigg(p(\underline{z}, t),\, s(\underline{z}, t),\, \frac{\partial p}{\partial t}, \,\ldots,\, \frac{\partial^i p}{\partial t^i},\, \nabla p,\, \ldots,\, \nabla^j p \bigg) \;=\; 0 \;\;,$$

where $s(\underline{z}, t)$ denotes the excitation generated by the phenomenon source to be located, and the operator $\nabla^j p$ is defined as $\nabla^j p := \frac{\partial p^j}{\partial z_x^j} + \frac{\partial p^j}{\partial z_y^j}$.

In model-based reconstruction, the considered linear partial differential equations are solved by using discretization methods. For spatial discretization, this paper employs the *finite-element-method* [9]. Temporal discretization is subsequently carried out by a *Crank-Nicolson* approach [10].

Spatial Discretization The finite-element-method transforms a distributed-parameter system given by a PDE into a lumped-parameter system in state-space form by employing spatial discretization. For spatially distributed phenomena, the solution $p(\underline{z}, t)$ of the characterizing PDE is expanded and subsequently replaced by a finite sum approximation of length D according to

$$p(\,\underline{z},\, t\,) \quad\approx\quad \sum_{i=0}^{D-1} \;\Phi_i(\,\underline{z}\,)\,\cdot\, x_i(\,t\,)\;\;. \tag{1}$$

This approximation separates the space-dependent analytic shape functions $\Phi_i(\underline{z})$ from time-dependent scaling factors $x_i(t)$. As a result, the spatially discretized solution is characterized by the vector $\underline{x}(t) := [x_0(t), x_1(t), \cdots, x_{D-1}(t)]^{\mathrm{T}}$ of scaling factors for each point of time t.

Temporal Discretization By applying the numerical stable Crank-Nicolson method for time discretization, the PDE can be converted into a system of ordinary differential equations (*ODE*). These ODEs then describe a physical phenomenon as a system in state-space form, governed by the system equation

$$\underline{x}_{k+1} \;=\; \mathbf{A}\cdot\underline{x}_k \;+\; \mathbf{B}\cdot\underline{s}_k \tag{2}$$

with system matrix $\mathbf{A}$. The discretized excitation $\underline{s}_k$ is tied to the system by means of an input matrix $\mathbf{B}$.

Model-Based Reconstruction Using equation (2) as a mathematical system model, it is now possible to reconstruct phenomenon values for any location $\underline{z}_n$ at arbitrary points of time t_k. Following equation (1), the state vector $\underline{x}_k$, i.e., the time discretized vector of scaling factors, and the vector $\underline{\Phi} := [\Phi_0, \Phi_1, \ldots, \Phi_{D-1}]$ of shape functions are employed to calculate the phenomenon value $p(\underline{z}_n, t_k)$ according to

$$p(\,\underline{z}_n,\, t_k\,) \;\;=\;\; \underline{\Phi}(\,\underline{z}_n\,)^T\cdot\underline{x}_k \;\;.$$

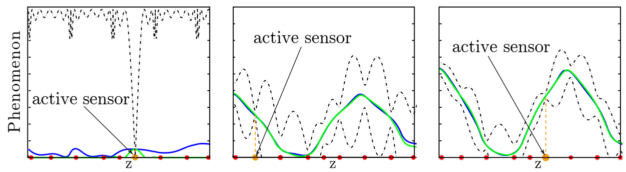

(a) $t_k = 1$ (b) $t_k = 14$ (c) $t_k = 20$

Figure 2: Model-based reconstruction (*green*) of a one-dimensional temperature distribution (*blue*) from discrete measurements (*orange*) of a distributed sensor network (*red*) as a stochastic state estimation with a 3-σ uncertainty bound (*black dashed*).

State Estimation The model-based reconstruction of a spatially distributed phenomenon from discrete space-time measurements now only requires to determine the phenomenon state vector $\underline{x}_k$ based on the acquired phenomenon values. In the chosen approach, this determination is implemented as a *stochastic state estimation* process utilizing the well-known Kalman filter. By interpreting the variables of (1) and (2) as random vectors and incorporating appropriate noise terms, these equations can be converted into their stochastic equivalents, which then serve as a measurement model and a system model in the employed estimator. The stochastic *system equation* is therefor given by

$$\underline{\boldsymbol{x}}_{k+1} \;=\; \mathbf{A} \cdot \underline{\boldsymbol{x}}_k \;+\; \mathbf{B}(\,\hat{\underline{s}}_k \;+\; \underline{\boldsymbol{w}}_k\,)\;,$$

where $\underline{\boldsymbol{x}}_k$ denotes the phenomenon state characterized as a Gaussian random vector and $\underline{\boldsymbol{w}}_k$ acts as white zero-mean Gaussian noise. Further on, the *measurement equation*, relating the phenomenon state $\underline{\boldsymbol{x}}_k$ to a measurement $\hat{y}_k^n$ at the sensor location $\underline{z}_n$ and the point of time t_k, is given by

$$\hat{y}_k^n \;=\; \mathbf{H}^n \cdot \underline{\boldsymbol{x}}_k \;+\; \boldsymbol{v}_k^n \;\;.$$

This equation incorporates a white zero-mean Gaussian noise source $\boldsymbol{v}_k^n$ and combines the different shape functions $\Phi_j(\underline{z})$ into a single measurement matrix $\mathbf{H}^n$ according to $\mathbf{H}^n := \underline{\Phi}(\underline{z}_n)^T = [\Phi_0(\underline{z}_n), \Phi_1(\underline{z}_n), \ldots, \Phi_{D-1}(\underline{z}_n)]^T$.

A more detailed description of the system conversion process and the stochastic state estimation can be found in [8]. An example for a model-based phenomenon reconstruction concludes this section. Figure 2 depicts the results of estimating a one-dimensional temperature distribution at different points of time t_k. It can be clearly seen how the reconstructed distribution (*green*) with elapsing time converges to the real temperature (*blue*). Furthermore, the reduction of estimation uncertainty, depicted as 3-σ-bound (*dashed black*), is obvious.

3 Source Localization

So far the reconstruction of spatially distributed phenomena was performed on the basis of a linear system model and on the assumption of a known excitation function. For a successful *localization of phenomenon sources*, the system model now has to be extended with an unknown excitation function. The extension approach considered in this paper is to define a set of parametric functions that characterize the excitation generated by a source in dependence on its current location $\underline{z}_k^{\mathrm{S}}$.

For modeling sources that generate excitation only in a spatially limited area, two parametric functions are considered. Punctuate sources are modeled by a Dirac delta function according to

$$s(\underline{z}, t) \;:=\; I(t)\,\delta(\underline{z} - \underline{z}_k^{\mathrm{S}}) \;\;,$$

where $I(t)$ denotes the source intensity at time t. Furthermore, sources with a limited spatial extension are mathematically represented as a Gaussian function

$$s(\underline{z}, t) \;:=\; I(t)\,\exp\left\{-\left(\underline{z} - \underline{z}_k^{\mathrm{S}}\right)^{\mathrm{T}} \begin{pmatrix} \xi_x & 0 \\ 0 & \xi_y \end{pmatrix} \left(\underline{z} - \underline{z}_k^{\mathrm{S}}\right)\right\}\;,$$

where the spatial extension of the source is determined by the two-dimensional width parameter $\underline{\xi} = [\xi_x, \xi_y]^{\mathrm{T}}$. Applying the aforementioned methods for spatial and temporal discretization to these continuous excitation functions results in a discrete excitation vector $\underline{s}(\underline{z}_k^{\mathrm{S}})$, which eventually constitutes a *non-linear function of the source location* $\underline{z}_k^{\mathrm{S}}$.

In source localization, the position of a source is not known a priori. In consequence, state estimation now has to cope with an unknown parameter, extending the model-based reconstruction of a continuous phenomenon to a *parameter estimation problem*. Thereby, the position of a source has to be estimated simultaneously to the reconstruction of the induced distributed phenomenon, based only on phenomenon values acquired by discrete sensor measurements.

State Augmentation A common approach to parameter estimation problems is state augmentation. In this paper, the former state vector $\underline{\boldsymbol{x}}_k$, representing the intrinsic phenomenon state, is augmented by a Gaussian random vector $\underline{\boldsymbol{z}}_k^{\mathrm{S}}$ representing the unknown source location $\underline{z}_k^{\mathrm{S}}$. The *augmented state vector* $\tilde{\underline{\boldsymbol{x}}}_k$ is then given by

$$\tilde{\underline{\boldsymbol{x}}}_k \;\;:=\;\; \left[\,\underline{\boldsymbol{x}}_k^{\mathrm{T}},\, (\underline{\boldsymbol{z}}_k^{\mathrm{S}})^{\mathrm{T}}\,\right]^{\mathrm{T}} \;\;.$$

As a consequence of this adjustment, the system models have to be augmented as well. Since the source location is considered to be unknown and no further information on the type of source movement is assumed to be given, the *movement of the source* over time is modeled as a random walk according to

$$\underline{\boldsymbol{z}}_{k+1}^{\mathrm{S}} \;=\; \underline{\boldsymbol{z}}_k^{\mathrm{S}} \;+\; \underline{\boldsymbol{w}}_k^{\mathrm{S}} \;\;,$$

where $\underline{\boldsymbol{w}}_k^{\mathrm{S}}$ denotes a white zero-mean Gaussian noise term. The respective *augmented system model* is then given by

$$\tilde{\underline{\boldsymbol{x}}}_{k+1} = \underbrace{\begin{bmatrix} \mathbf{A} & \mathbf{0} \\ \mathbf{0} & \mathbf{I}_2 \end{bmatrix} \cdot \tilde{\underline{\boldsymbol{x}}}_k + \begin{bmatrix} \mathbf{B} & \mathbf{0} \\ \mathbf{0} & \mathbf{I}_2 \end{bmatrix} \left(\begin{bmatrix} \underline{s}(\underline{\boldsymbol{z}}_k^{\mathrm{S}}) \\ \underline{0} \end{bmatrix} + \begin{bmatrix} \underline{\boldsymbol{w}}_k \\ \underline{\boldsymbol{w}}_k^{\mathrm{S}} \end{bmatrix} \right)}_{=:\, \underline{a}_k(\tilde{\underline{\boldsymbol{x}}}_k)}\,, \quad (3)$$

with $\mathbf{I}_2$ denoting the two-dimensional identity matrix. Due to the fact that the excitation vector depends upon the unknown source location in a non-linear manner, the state augmentation results in a *non-linear system model*. Thus, state estimation gets more complicated, since it can no longer be performed by a linear Kalman filter.

The stochastic state estimation process generally consists of two processing steps performed in an alternating fashion. In the prediction step, the evolution of the system state over time is determined based on the considered system model. In the filter step, acquired measurement values are incorporated into the state estimate via Bayesian fusion. Both processing steps result in a multi-variate density function representing the estimate of the system state. For the considered source localization problem, the evolution of the augmented system state $\underline{\tilde{\boldsymbol{x}}}_k$ is characterized by the non-linear system equation (3). For such non-linear system models, a closed-form calculation of the corresponding density functions is not possible in general.

Gaussian Filters As a solution to this problem, approximation techniques can be applied. Thereby, two alternate approaches exist. In the first approach, the non-linear system model is approximated by linear equations. The well-known extended Kalman filter follows this approach. Alternatively, it is possible to approximate the predicted state density function. This latter approach is implemented by a class of estimators known as *Gaussian filters* or linear regression Kalman filters, respectively. Gaussian filters, such as the unscented Kalman filter [11], approximate the predicted system state by propagating deterministically chosen sampling points through the non-linear system model.

This Gaussian filter approach is illustrated in Figure 3. First, a given Gaussian density function representing the system state $\underline{\boldsymbol{x}}_k$ is deterministically approximated by a number of weighted sigma points $\underline{x}_k^{(i)}$ with weights ω_i. These sigma points are then propagated through the non-linear system model $\underline{a}_k(\,\cdot\,)$, resulting in the predicted sigma points $\underline{x}_{k+1}^{(i)} = \underline{a}_k(\underline{x}_k^{(i)})$. Based on these sigma points, an approximate density function of the predicted system state $\underline{\boldsymbol{x}}_{k+1}$ can be determined. For this purpose, the predicted mean $\underline{\hat{x}}_{k+1}$ and covariance $\mathbf{C}_{k+1}^x$ are calculated according to

$$\begin{aligned} \underline{\hat{x}}_{k+1} &:= \sum_i \omega_i \cdot \underline{x}_{k+1}^{(i)} \;, \\ \mathbf{C}_{k+1}^x &:= \sum_i \omega_i \left(\underline{x}_{k+1}^{(i)} - \underline{\hat{x}}_{k+1}\right)\left(\underline{x}_{k+1}^{(i)} - \underline{\hat{x}}_{k+1}\right)^{\mathrm{T}} . \end{aligned} \tag{4}$$

Gaussian Estimator In this paper, the *Gaussian Estimator* proposed in [12] is employed as basis for state estimation and sensor management. In contrast to most of the existing linear Kalman regression filters, the Gaussian Estimator allows an adjustable number L of sigma points. Hence, the Gaussian Estimator is able to capture not only higher order moments of the original density function, but consequently more information of the non-linear system equation as well.

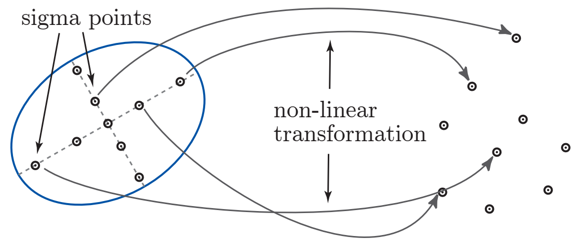

Figure 3: Density approximation and prediction step of a Gaussian filter.

Since parts of this approximation are performed off-line, the Gaussian Estimator constitutes both an accurate and computationally efficient state estimator well-suited for a source localization and tracking task.

A further reduction of computational complexity is possible by applying techniques like Rao-Blackwellization. Following the approach proposed in [13] enables the exploitation of existing linear substructures in the considered system equations. Basically, this approach allows to treat linear and non-linear parts separately. The resulting conditional linear state dimensions can then be processed by a Kalman filter, which significantly reduces the overall computational demand and simultaneously enhances the estimation accuracy. This extension of the Gaussian Estimator eventually allows for a real-time localization of movable sources.

Gaussian Mixture Estimator In the case of non-linear transformations, the processing steps in state estimation change the type of density functions. Gaussian density functions are thereby transformed into arbitrarily shaped functions, like multi-modal or skewed densities. To handle this problem, the system state $\underline{\boldsymbol{x}}_k$ has to be represented by a class of density functions that are both easy to handle and able to capture (or at least approximate) arbitrary density functions.

A *Gaussian mixture* representation is one way of fulfilling these requirements. A Gaussian mixture or Gaussian sum [14] is thereby given as a weighted sum $f(\underline{x}) := \sum_{i=1}^G \eta_i \; \mathcal{N}(\underline{x} - \underline{\hat{x}}_i, \mathbf{C}_i^x)$ of G separate Gaussian density functions $\mathcal{N}(\underline{x} - \underline{\hat{x}}_i, \mathbf{C}_i^x)$ with mean $\underline{\hat{x}}_i$, covariance matrice $\mathbf{C}_i^x$ and non-negative weight η_i.

In this paper, a *Gaussian Mixture Estimator* [12] is employed for non-linear state estimation. This estimator basically applies the previously introduced Gaussian Estimator to each component of a given Gaussian mixture. In addition to this processing of the individual means and covariances, the weights $\eta_{i,k}$ have to be updated in each time step t_k as well. For this purpose, the computationally feasible approximative approach proposed in [14] was chosen. In this approach, at the filter step the individual weighting factors

$$\gamma_{i,k} \quad = \quad \mathcal{N}\Big(\, \underline{\hat{y}}_k \,-\, \mathbf{H}\,\underline{\hat{x}}_{i,k}^p ,\; \mathbf{H}\,\mathbf{C}_{i,k}^{x,p}\,\mathbf{H}^{\mathrm{T}} \,+\, \mathbf{C}_k^v \Big)$$

are calculated based on the predicted Gaussian mixture means $\underline{\hat{x}}_{i,k}^p$ and covariances $\mathbf{C}_{i,k}^{x,p}$ as well as the current measurements $\underline{\hat{y}}_k$. These weighting factors are then used for

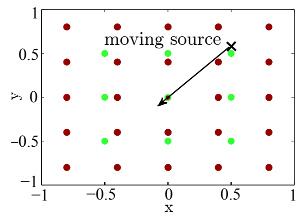

(a) Stationary sensor network consisting of 9 (*green*), 25 (*red*) sensor nodes and moving source (*black*).

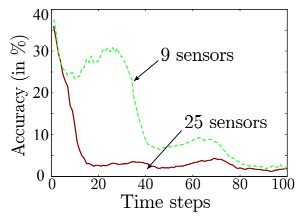

(b) Percental localization accuracy for measurements by 9 (*green*) and 25 (*red*) sensor nodes.

Figure 4: Model-based source localization and tracking.

updating the weights of the previous time step according to $\eta_{i,k} = \gamma_{i,k} \cdot \eta_{i,k-1}$.

Proof of concept As a proof of concept, source localization was performed by means of simulation. Considering sources of plane air or water contaminations as well as sources of plane temperature distributions, the induced distributed phenomenon $p(\underline{z}, t)$ was modeled by the two-dimensional advection-diffusion-equation

$$\frac{\partial p}{\partial t} + u_x \cdot \frac{\partial p}{\partial z_x} + u_y \cdot \frac{\partial p}{\partial z_y} - c \cdot \left(\frac{\partial^2 p}{\partial z_x^2} + \frac{\partial^2 p}{\partial z_y^2} \right) = I(t) \cdot \exp\left\{ - \left(\underline{z} - \underline{z}_k^{\mathrm{S}} \right)^{\mathrm{T}} \begin{pmatrix} \xi_x & 0 \\ 0 & \xi_y \end{pmatrix} \left(\underline{z} - \underline{z}_k^{\mathrm{S}} \right) \right\} ,$$

with advection velocity $\underline{u} := [u_x, u_y]^{\mathrm{T}}$ and diffusion coefficient c. In simulation, the constant values of $\underline{u} = [-5, -8]^{\mathrm{T}}$ and $c = 1$ were applied to the phenomenon, and a small Gaussian source with a constant intensity $I = 1500$ and width $\underline{\xi} = [0.1, 0.1]^{\mathrm{T}}$ was considered. This source was able to move within a confined area normalized to the square $[-1, 1] \times [-1, 1]$, as illustrated in Figure 4(a).

To acquire the induced distributed phenomenon, two stationary sensor network configurations were simulated, consisting of $N = 9$ and $N = 25$ sensors, respectively, as depicted in Figure 4(a) as well. Thereby, all the nodes of the chosen configuration simultaneously performe measurements at each time step. These measurements were perturbed by a measurement noise of $\mathbf{C}_v = 0.01 \cdot \mathbf{I}_N$, with $\mathbf{I}$ denoting the identity matrix. For tracking the source location, the previously derived non-linear system model (3) with a system noise $\mathbf{C}_w = 0.1 \cdot \mathbf{I}_{D+2}$ was incorporated into the Gaussian Mixture Estimator.

The tracking results for an observation period of $M = 100$ time steps are displayed in Figure 4(b). For both considered sensor networks, the suggested localization methods were able to accurately locate and track a moving phenomenon source in real-time, i.e., with a runtime lower than 1 second per time step. As can be further seen, a larger number of sensors indeed leads to a better rate of convergence in source position. But in the long run, the localization accuracy is similar for both sensor networks.

4 Sensor Management

In the last section, methods for locating and tracking movable sources of continuous physical phenomena by distributed sensing systems have been introduced. In the following section, *sensor management* techniques are proposed for increasing the information gain of acquired measurements in source localization.

Sensor Management In application scenarios, distributed sensor systems are often subject to resource restrictions. Self-sufficient nodes in sensor networks, for example, are subject to energy constraints and therefore require a careful usage for prolonging the overall life-time of the network. On the other hand, mobile sensors may be at hand only in small numbers for cost reasons. In consequence, the proposed source localization methods must be able to perform well even with a reduced number of sensors. However, as yet indicated by Figure 4(b), an unelaborate reduction of sensor measurements leads to a significant loss of accuracy. Thus, for accurate localization results a sophisticated selection of measurement locations is required.

A general solution to optimal control of measurement systems is provided by *sensor management*. Sensor management thereby aims at maximizing the information gain of sensor measurements in presence of resource restrictions. Given a finite set of possible sensor configurations $\mathcal{U}_C$, sensor management determines the configuration $\underline{u}_k \in \mathcal{U}_C$ resulting in the maximum information gain. In the case of source localization by means of a mobile sensor, each configuration moves the sensor to a specific location, given the current sensor position. For a given observation period of length M, multi-step (or non-myopic) sensor management aims at maximizing the localization accuracy resulting from applying a sequence of sensor measurements. Thereby, an optimal sequence $\underline{u}^*_{0:M-1}$ of sensor configurations is determined by minimizing a chosen quality criterion $\mathrm{G}(\,\cdot\,)$ over all possible configuration sequences $\underline{u}_{0:M-1} := (\underline{u}_0, \underline{u}_1, \ldots, \underline{u}_{M-1})$ of length M according to

$$\underline{u}^*_{0:M-1} = \arg\min_{\underline{u}_{0:M-1}} \left(\mathrm{G}(\, \underline{u}_{0:M-1} \,) \right) .$$

The localization accuracy resulting from applying a specific configuration sequence in general depends on future measurement values that are unavailable at processing time. The quality criterion $\mathrm{G}(\,\cdot\,)$ therefore is employed to predict the resulting localization accuracy based on a current state estimate $\underline{\boldsymbol{x}}_k$, thus allowing to compare configuration sequences prior to measuring. In this paper, a *covariance-based quality criterion* is utilized, judging localization accuracy in terms of the remaining uncertainty of the predicted state estimate, e.g., by means of trace

$$\mathrm{G}(\, \underline{u}_{0:k} \,) := \mathrm{trace}\left(\mathbf{C}_k^z \left(\underline{u}_{0:k} \right) \right) ,$$

where $\mathbf{C}_k^z\left(\underline{u}_{0:k}\right)$ is the covariance matrix of the estimated source location $\underline{\boldsymbol{z}}_k^{\mathrm{S}}$ at time step t_k given the sequence $\underline{u}_{0:k}$.

Quasi-Linear Sensor Management How to calculate a predicted state estimate that allows for a reasonable choice

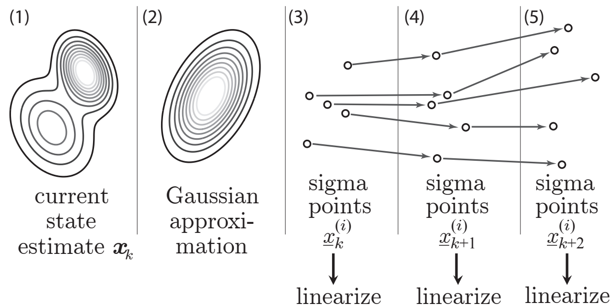

Figure 5: Calculation of the linearization trajectory for quasi-linear sensor management [12].

of sensor configurations is one of the central questions of sensor management. In this paper, the quasi-linear approach [12] to the sensor management problem in source localization is considered. This approach is based on management techniques applicable in the case of linear system models perturbed by Gaussian noise.

In *linear sensor management*, the evolution of a covariance-based quality criterion over a given observation period can be determined both a priori and independently from actual measurement values [15]. The evolution of state covariance $\mathbf{C}_k^x$ for a sensor configuration $\underline{u}_k$ is thereby characterized by the recursive algebraic Riccati equation

$$\mathbf{C}_{k+1}^x(\underline{u}_k) = \mathbf{A}_k \mathbf{C}_k^x \mathbf{A}_k^{\mathrm{T}} + \mathbf{B}_k \mathbf{C}_k^w \mathbf{B}_k^{\mathrm{T}} - \mathbf{A}_k \mathbf{K}_k^u \mathbf{H}_k^u \mathbf{C}_k^x \mathbf{A}_k^{\mathrm{T}} \ ,$$

with $\mathbf{K}_k^u$ denoting the Kalman gain as a function of the sensor configuration $\underline{u}_k$. For choosing an optimal configuration sequence, the Riccati equation merely has to be evaluated for all possible configuration sequences with respect to the considered observation period. This basically can be done by searching the *tree of possible configuration sequences* with a depth of M and a branching factor of $|\mathcal{U}_C|$.

By utilizing pruning algorithms in tree search, linear sensor scheduling can be implemented in an efficient manner [16]. Furthermore, *model predictive control* techniques [17] allow to balance the computational burden of a tree search against the gain of estimation quality resulting from sensor management. In this paper, model predictive control is implemented by a receding scheduling horizon P. In each time step t_k, only short configuration sequences $u_{k:k+P-1}$ of a length $P < M$ have to be considered in tree search. This approach then even allows for performing a sophisticated sensor management under real-time constraints.

In the case of *non-linear systems*, sensor management is clearly more complicated. The main difficulty in non-linear sensor management is caused by the fact that here the evolution of the quality criteria is no longer independent of future measurements. A possible way to handle this problem is given by approximating the considered non-linear systems by linear equations. This approach, implemented in *quasi-linear sensor management*, allows for extending the advantages of linear sensor management to non-linear systems.

Basically, quasi-linear sensor management applies a technique called statistical linearization for system approximation, which happens to be the same technique as employed in the Gaussian Estimator. For one time step, statistical linearization is independent of measurement values, which is the key for implementing an efficient linear sensor management approximation to the given non-linear management problem in source localization.

The basic idea of *predictive statistical linearization* is depicted in Figure 5. Here, the predicted system state $\underline{\boldsymbol{x}}_{k+j}$ is calculated for all scheduling time steps t_{k+j} in the considered scheduling horizon $j \in \{1, 2, \ldots, P\}$ by means of a so-called linearization trajectory of sigma points. Beginning with the current system state $\underline{\boldsymbol{x}}_k$, the state density function (**1**) is approximated by a Gaussian density function (**2**) and is then represented by means of a set of weighted sigma points $\{\omega_{i,k},\, \underline{x}_k^{(i)}\}$ (**3**). Recursively propagating the sigma points $\{\omega_{i,k+j},\, \underline{x}_{k+j}^{(i)}\}$ through the non-linear system equation at each scheduling time step t_{k+j} results in the desired linearization trajectory (**3**-**5**). Based on this trajectory of sigma points, the non-linear system equation (and a non-linear measurement equation if necessary) is linearized separately for each scheduling time step by statistical linearization.

Statistical linearization itself approximates a non-linear transformation of random variables given by $\underline{\boldsymbol{y}} = \underline{\mathrm{g}}(\underline{\boldsymbol{x}})$ via a linear equation $\underline{\boldsymbol{y}} \approx \mathbf{A} \cdot \underline{\boldsymbol{x}} + \underline{b}$. For this purpose, the non-linear transformation $\underline{\mathrm{g}}(\,\cdot\,)$ is evaluated for a set of weighted sigma points $\{\omega_i,\, \underline{x}_i\}$, resulting in transformed sigma points $\underline{y}_i$ with unaltered weights ω_i. By minimizing the sum of squared errors

$$\{\mathbf{A},\, \underline{b}\} \;=\; \arg\min_{\tilde{\mathbf{A}},\tilde{\underline{b}}} \sum_i \omega_i \Big(\underline{y}_i - \tilde{\mathbf{A}}\underline{x}_i - \tilde{\underline{b}}\Big)^{\mathrm{T}} \Big(\underline{y}_i - \tilde{\mathbf{A}}\underline{x}_i - \tilde{\underline{b}}\Big)$$

between the linear and non-linear transformation for all sigma points, the matrix $\mathbf{A}$ and the vector $\underline{b}$ can be determined. The solution to this equation is then given by

$$\mathbf{A} \;=\; \mathbf{C}_{xy}^{\mathrm{T}} \cdot \mathbf{C}_x^{-1} \ , \qquad \underline{b} \;=\; \hat{\underline{y}} - \mathbf{A} \cdot \hat{\underline{x}} \ ,$$

where the means $\hat{\underline{x}}$, $\hat{\underline{y}}$ and the covariances $\mathbf{C}_x$, $\mathbf{C}_y$ are calculated according to (4). The cross-covariance $\mathbf{C}_{xy}$ is given by $\mathbf{C}_{xy} = \sum_i \omega_i \big(\underline{x}_i - \hat{\underline{x}}\big)\big(\underline{y}_i - \hat{\underline{y}}\big)^{\mathrm{T}}$. As a result, the linearized transformation is then given by $\underline{\boldsymbol{y}} = \mathbf{A} \cdot \underline{\boldsymbol{x}} + \underline{\bar{\boldsymbol{w}}}$, where $\underline{\bar{\boldsymbol{w}}}$ denotes an additional system noise with mean and covariance matrix

$$\hat{\underline{\bar{w}}} \;=\; \hat{\underline{y}} - \mathbf{A} \cdot \hat{\underline{x}} \;=\; \underline{b} \ , \qquad \mathbf{C}^{\bar{w}} \;=\; \mathbf{C}^y - \mathbf{A}\,\mathbf{C}^x \mathbf{A}^{\mathrm{T}}$$

corresponding to the linearization error.

In summary, a quasi-linear sensor manager recursively performs the following tasks at each time step t_k:

1. predictive statistical linearization over a given scheduling horizon P,
2. solve the linear sensor management problem,
3. apply the first sensor configuration $\underline{u}_k$ and perform a measurement,
4. perform (non-linear) state estimation via the Gaussian Mixture Estimator and go back to 1.

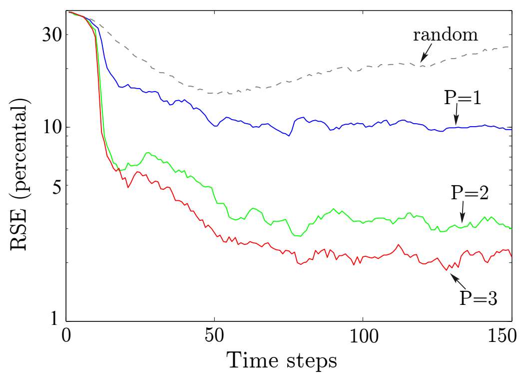

Figure 6: Percental localization accuracy in model-based source localization for four different scheduling horizons.

Localization Results Concluding this section, the results of a simulated source localization and tracking by a *single mobile sensor* controlled by a *quasi-linear sensor manager* are presented. For this purpose, the setup described in Section 3 was re-used, now with an observation period of $M = 150$ time steps. The mobile sensor has differential-drive kinematics and is controlled by setting its current steering angle to one of five possible configurations with $\mathcal{U}_c = \{\frac{i\pi}{6} | i = -2, \ldots, 2\}$. After changing its orientation accordingly, the sensor moves along the new direction with a linear velocity of $v^M = 20$. In addition, the sensor is able to measure without moving.

In Figure 6 the localization accuracy for an estimated source location $\underline{z}_k^{\mathrm{S}}$ and a real source location $\hat{\underline{z}}_k^{\mathrm{S}}$ is depicted in terms of the mean percental root square error

$$\mathrm{RSE}(\underline{z}_k^{\mathrm{S}}) := \sum_{i=1}^{N} \frac{100}{N \cdot d} \sqrt{\left(\underline{z}_{k,i}^{\mathrm{S}} - \hat{\underline{z}}_{k,i}^{\mathrm{S}}\right)^{\mathrm{T}} \cdot \left(\underline{z}_{k,i}^{\mathrm{S}} - \hat{\underline{z}}_{k,i}^{\mathrm{S}}\right)}$$

with respect to the side length d of the observation area, calculated over N=100 Monte Carlo simulation runs. Thereby, three different receding scheduling horizons of length 1 to 3 and a random sensor selection were considered. It is obvious that a single mobile sensor controlled by sensor management in this setup is able to perform nearly as good as a stationary sensor network consisting of 25 simultaneously active nodes. The actual performance thereby depends on the scheduling horizon P, i.e., the longer the horizon, the more accurate the localization. A more detailed performance statistic is given in Table 1.

Figure 7 furthermore depicts two exemplary trajectories representing the movement of the mobile sensor and the source movement for the two scheduling horizons $P = 1$ and $P = 3$. For both horizons, the sensor sparsely monitors a wide portion of the observed area at the beginning. In this phase, the sensor sometimes stalls its movement when no informative measurements are available. The sensor trajectories significantly differ at this phase for different horizon lengths. For $P = 1$, the sensor moves almost orthogonal to the source. Due to the short horizon, the sensor is not able to anticipate the future movement of the source. In contrast, for a longer horizon of $P = 3$, the sensor is able to track the path of the source more accurately. In a second phase, when estimation uncertainty decreases (or equivalent: localization accuracy increases), the sensor circles (due to its higher velocity) the source in order to uniformly monitor the phenomenon over a broad region. This behavior further improves the localization accuracy and is more pronounced for $P = 3$. It is important to note, that the sensor follows the center of the induced phenomenon, which lies *behind* the moving source due to the adversely directed advection.

P	runtime	good runs	Ø RSE	stable acc.
rand.	< 0.1s	74%	21.5%	12%
1	0.2s	90%	13.4%	10%
2	0.9s	98%	6.5%	3%
3	4.4s	100%	5.3%	2%

Table 1: Source localization by a mobile sensor controlled by quasi-linear sensor management. Depicted are runtime for one management step, the number of good runs, i.e., runs where the sensor was able to follow the source, the percental RSE averaged over the complete observation period and the stable accuracy reach after 100 time steps.

5 Conclusions and Future Work

In this paper, a novel method was presented for localizing, tracking, and pursuing movable sources of spatially distributed phenomena by either a stationary network of sensor nodes or a team of mobile sensors. The proposed approach is characterized by the following properties:

- The *numerically* solved *model-based approach* enables a recursive processing scheme in combination with low measurement rates.
- *Stochastic estimators* allow for *continually quantifying* the resulting *localization accuracy* by means of estimation uncertainty.
- The Gaussian Mixture Estimator enables a computationally efficient recursive *localization of moving phenomenon sources*.
- Efficient *sensor management methods* allow for a real-time *tracking and pursuing of phenomenon sources* in a continuous manner by mobile sensors and further facilitate an *accurate source localization* with a limited number of (active) sensor nodes.

Future works is devoted to an extended parameter estimation, allowing for additionally estimating phenomenon parameters such as advection velocity or diffusion coefficients as well as the source intensity simultaneously to source localization. A further subject of future work is the task of locating multiple sources.

References

[1] Ian F. Akyildiz, Su Weilian, Yogesh Sankarasubramaniam, and Erdal Cayirci, "A Survey on Sensor Networks," *IEEE Communications Magazine*, vol. 40, pp. 102–114, Aug. 2002.

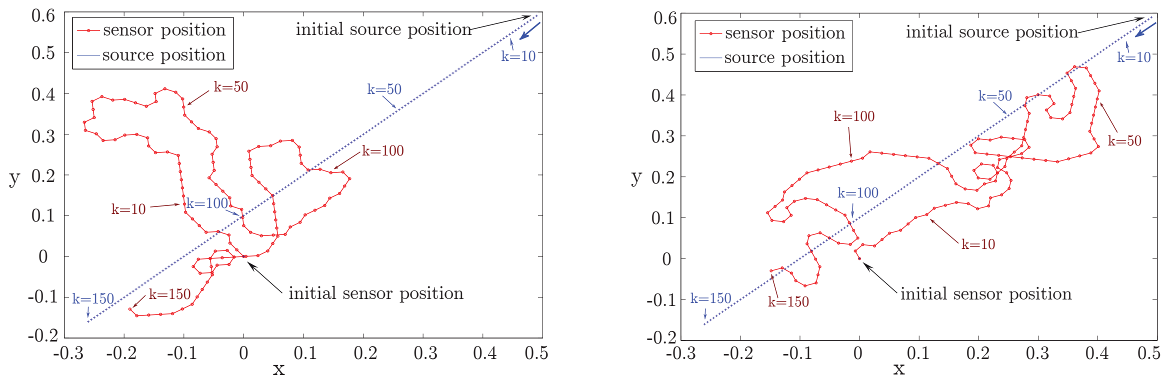

(a) Trajectory for a scheduling horizon $P = 1$.

(b) Trajectory for a scheduling horizon $P = 3$.

Figure 7: Source trajectories (blue) and mobile sensor trajectories (red) in model-based source localization.

[2] Mehmet E. Alpay and Molly H. Shor, “Model-based Solution Techniques for the Source Localization Problem,” *IEEE Transactions on Control Systems Technology*, vol. 8, pp. 895–904, 2000.

[3] Jörg Matthes, Lutz Gröll, and Hubert B. Keller, “Source localization by spatially distributed electronic noses for advection and diffusion,” *IEEE Transactions on Signal Processing*, vol. 53, no. 5, pp. 1711–1719, 2005.

[4] Michael A. Demetriou, “Power management of sensor networks for detection of a moving source in 2-D spatial domains,” in *Proceedings of the 2006 American Control Conference*, Minneapolis, Minnesota, USA, Jun. 2006, pp. 1144–1149.

[5] Maciej Patan and Dariusz Uciński, “Optimal scheduling of mobile sensor networks for detection and localization of stationary contamination sources,” in *Proceedings of the 11th International Conference on Information Fusion (Fusion 2008)*, Cologne, Germany, Jul. 2008, pp. 366–372.

[6] Boaz Porat and Arye Nehorai, “Localizing Vapor-Emitting Sources by Moving Sensors,” in *Conference Record of the Twenty-Eighth Asilomar Conference on Signals, Systems and Computers*, vol. 2, Oct. 1994, pp. 765–769.

[7] Felix Sawo, *Nonlinear State and Parameter Estimation of Spatially Distributed Systems*. Ph.D. Thesis, Universität Karlsruhe (TH), 2009.

[8] Felix Sawo, Kathrin Roberts, and Uwe D. Hanebeck, “Bayesian Estimation of Distributed Phenomena using Discretized Representations of Partial Differential Equations,” in *Proceedings of the 3rd International Conference on Informatics in Control, Automation and Robotics (ICINCO 2006)*, Setúbal, Portugal, Aug. 2006, pp. 16–23.

[9] Andrew J. Baker, *Finite Element Computational Fluid Mechanics*. Taylor and Francis, 1983.

[10] John Crank and Phyllis Nicolson, “A practical method for numerical evaluation of solutions of partial differential equations of the heat-conduction type,” *Advances in Computational Mathematics*, vol. 6, no. 1, pp. 207–226, 1996.

[11] Simon J. Julier and Jeffrey K. Uhlmann, “A new extension of the kalman filter to nonlinear systems,” in *International Symposium on Aerospace/Defense Sensing, Simulation and Controls (SPIE)*, Orlando, Florida, USA, 1997.

[12] Marco Huber, *Probabilistic Framework for Sensor Management*. Ph.D. Thesis, Universität Karlsruhe (TH), 2009.

[13] Frederik Beutler, Marco F. Huber, and Uwe D. Hanebeck, “Gaussian Filtering using State Decomposition Methods,” in *Proceedings of the 12th International Conference on Information Fusion (Fusion 2009)*, Seattle, Washington, USA, Jul. 2009.

[14] Daniel L. Alspach and Harold W. Sorenson, “Nonlinear bayesian estimation using gaussian sum approximations,” *IEEE Transactions on Automatic Control*, vol. 17, pp. 438–448, 1972.

[15] Lewis Meier, III, John Peschon, and Robert M. Dressler, “Optimal control of measurement subsystems,” *IEEE Transactions on Automatic Control*, vol. 12, no. 5, pp. 528–536, Oct. 1967.

[16] Marco F. Huber and Uwe D. Hanebeck, “Priority List Sensor Scheduling using Optimal Pruning,” in *Proceedings of the 11th International Conference on Information Fusion (Fusion 2008)*, Cologne, Germany, Jul. 2008.

[17] Manfred Morari and Jay H. Lee, “Model Predictive Control: Past, Present and Future,” *Computers and Chemical Engineering*, 1997.